Supporting Information: Dynamic Polymer Nanocomposites Towards Strain Sensors and Customizable Resistors

Obed J. Dodo,† Ibrahim O. Raji,† Ian J. Arny,† Camryn P. Myers,† Leilah Petit,† Kumari Walpita,† Derrick Dunn,† Carl J. Thrasher,¶ Dominik Konkolewicz†*

†*Department of Chemistry and Biochemistry, Miami University, 651 East High Street, Oxford, OH 45056, USA.*

¶*Department of Materials Science and Engineering, Massachusetts Institute of Technology, Cambridge, MA 02142, USA*

*Email: d.konkolewicz@miamioh.edu

1. Analytical Methods and Characterization

Nuclear Magnetic Resonance (NMR)

NMR experiments were performed on Bruker Advance 400 MHz spectrometer using $CDCl_3$ as solvent at 298 K.

Determination of Monomer Conversion by ^{1}H-NMR

Conversion was determined using NMR by integrating the sum of polymerized and unpolymerized ethyl acrylate [4.4-4.0 ppm] against the vinyl protons at 6.5, 6.1 and 5.8 ppm. Consumption of FMA and Upy was found to be near quantitative in each case by NMR (Table S1).

Size exclusion Chromatography (SEC)

Molecular weights and dispersities were determined using an Agilent 1260 SEC system equipped with an autosampler, an Agilent 1260 isocratic pump, Agilent 1 guard and 2 analytical Polar Gel-M columns, degasser, and Agilent 1260 refractive index [RI detector] and a viscometer for universal calibration. N,N-dimethylformamide (DMF) + 0.1 wt.% LiBr was used as the eluent with a flow rate of 1 mL/min at 25 °C. The system was calibrated with poly[methyl methacrylate] standards with molecular weights the range of 617500 to 1010. All samples were filtered through a 200 nm PTFE filter prior to injection.

Instron Tensile Testing

An Instron 3344 universal testing system equipped with a 100 N load cell was used to conduct tensile testing of the materials at room temperature to obtain stress-strain curve. The extension was increased at a rate of 0.5 mm/s. In all cases, data was collected until specimen failure. Each tensile test was repeated at least twice.

Frequency Sweep

All frequency sweep experiments were performed using isothermal frequency sweep test method on TA instrument DMA Q800 equipped with a tension clamp. Frequency ranged from 0.01- 100 Hz at constant temperatures of 25, 45, and 65 °C. A strain of 0.3% and a preload force of 0.01 N was applied.

Stress Relaxation

Stress relaxation was performed on a TA instrument DMA Q800 equipped with the tension film clamp. A constant strain of 10% was maintained on the material for 4 hours at 30 °C and the relative stress was recorded.

Differential Scanning Calorimetry (DSC)

All glass transition temperatures [T_g] were obtained using TA instrument DSC Q2000. The data was obtained in a heat cool heat cycle ranging from -50 °C to 150 °C with 10 °C/min heating rate. Data from the second heating cycle was used to plot the curve. The DSC experiment was carried out twice for reproducibility.

Thermogravimetric Analysis (TGA)

All TGA data were obtained using a TA instrument TGA Q500. Experiments were performed using a heating rate of 10 °C/min in the range of 35 °C to 400 °C under nitrogen with a flow rate of 40 mL/min.

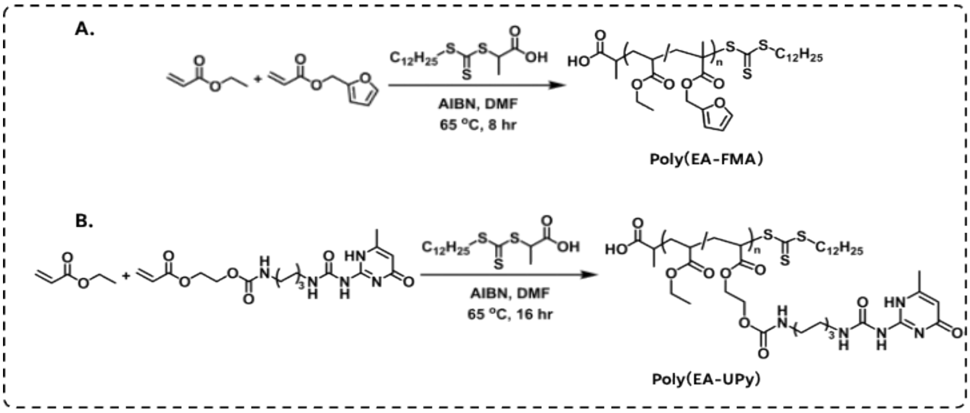

Scheme S1. (**A**) Synthesis of Poly(EA-FMA) and (**B**) Poly(EA-UPy) precursors for IPNs.

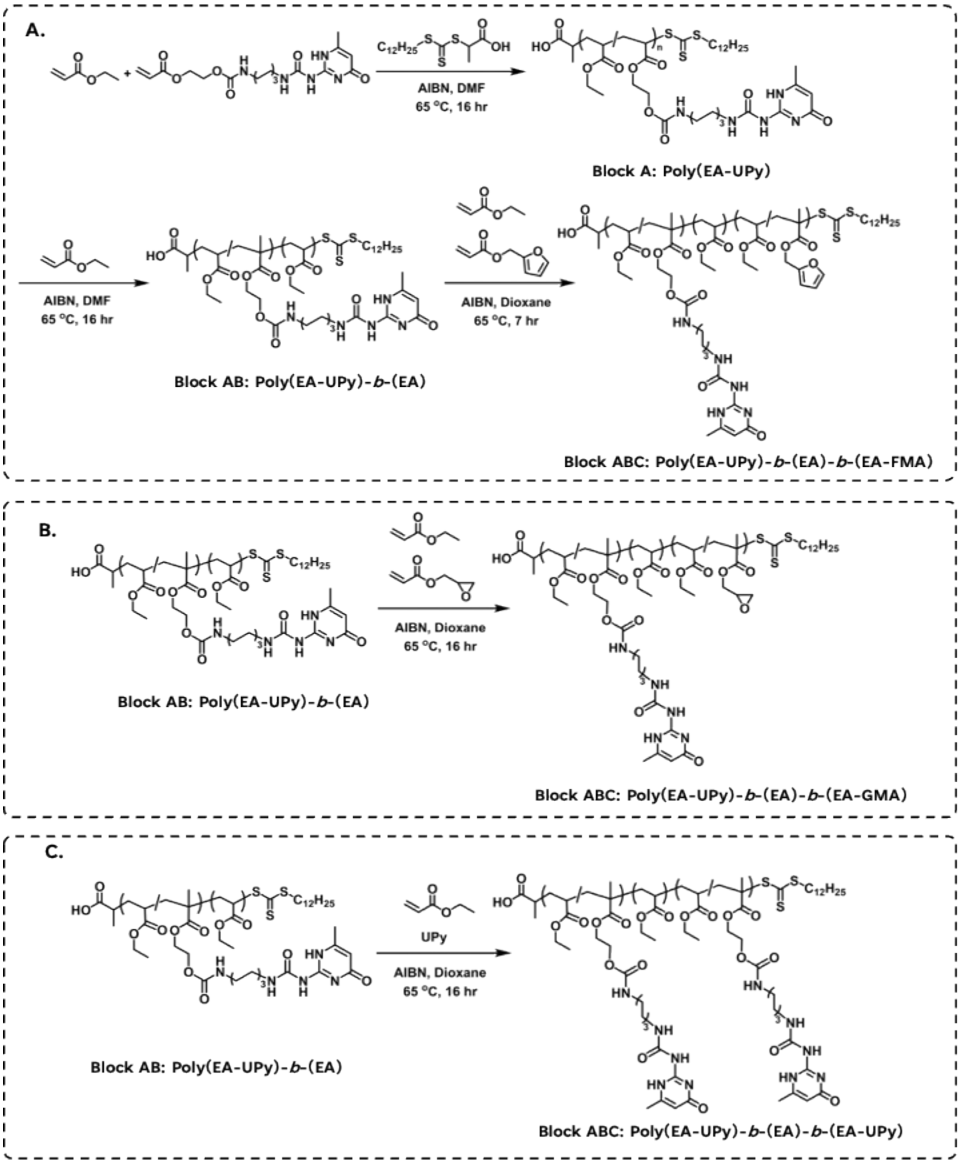

Scheme S2. Synthesis of BCN-based (**A**) ABC-type Poly(EA-UPy)-*b*-(EA)-*b*-(EA-FMA) for DPN7, (**B**) ABC-type Poly(EA-UPy)-*b*-(EA)-*b*-(EA-GMA) for DPN8, and (**C**) ABA-type Poly(EA-UPy)-*b*-(EA)-*b*-(EA-UPy) for DPN6 block copolymers using RAFT polymerization.

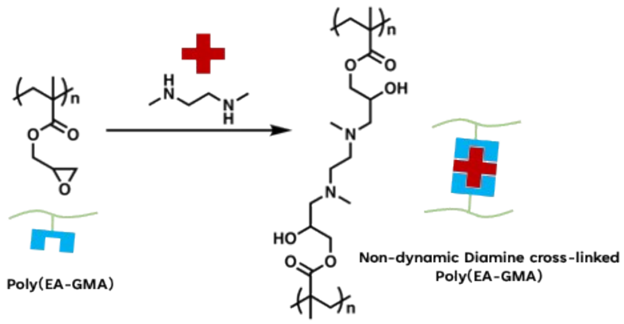

Scheme S3. Cross-linking of ABC-type Poly(EA-UPy)-*b*-(EA)-*b*-(EA-GMA) block copolymers is achieved through dynamic quadrupole Hydrogen bonding and through epoxy ring-opening reaction using N,N'-dimethylethylenediamine as shown above. The resulting diamine cross-links are not dynamic, hence resulting in poor dynamic properties (e.g., self-healing) for Poly(EA-UPy)-*b*-(EA)-*b*-(EA-GMA) as shown in Figure 2.

2. Supplemental Data

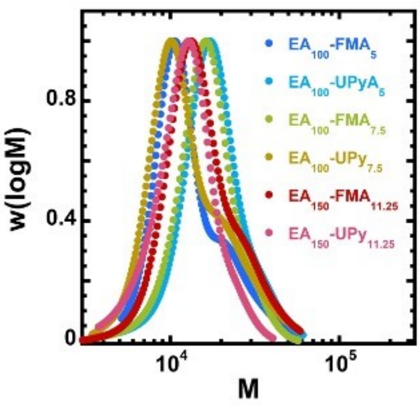

Figure S1. GPC traces of IPN precursors: poly(EA_{100}-FMA_5), poly(EA_{100}-UPy_5), poly(EA_{100}-$FMA_{7.5}$), poly(EA_{100}-$UPy_{7.5}$), poly(EA_{150}-$FMA_{11.25}$), and poly(EA_{150}-$UPy_{11.25}$). Dispersity data is provided in Table S1.

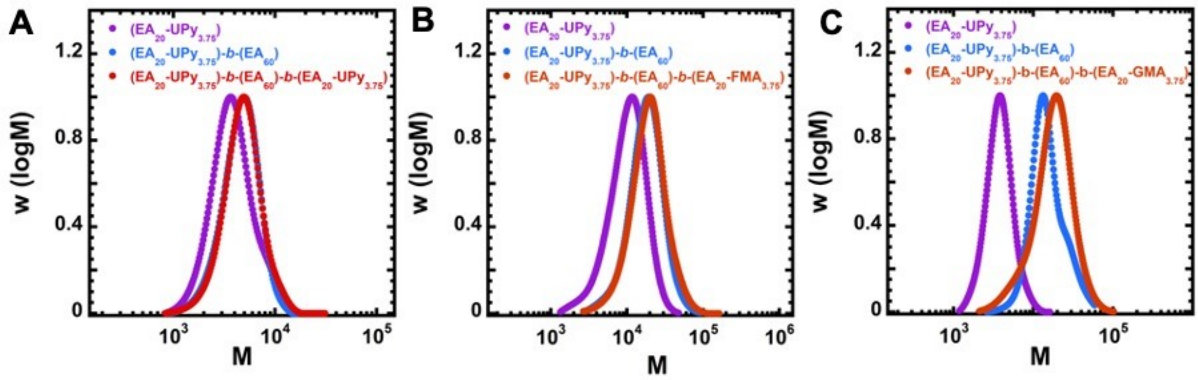

Figure S2. GPC traces of BCN precursors and polymers: (**A**) Poly(EA_{20}-$UPy_{3.75}$), Poly(EA_{20}-$UPy_{3.75}$)-*b*-(EA_{60}), and Poly(EA_{20}-$UPy_{3.75}$)-*b*-(EA_{60})-*b*-(EA_{20}-$UPy_{3.75}$). (**B**) Poly(EA_{20}-$UPy_{3.75}$), Poly(EA_{20}-$UPy_{3.75}$)-*b*-(EA_{60}), and Poly(EA_{20}-$UPy_{3.75}$)-*b*-(EA_{60})-*b*-(EA_{20}-$FMA_{3.75}$). (**C**) Poly(EA_{20}-$UPy_{3.75}$), Poly(EA_{20}-$UPy_{3.75}$)-*b*-(EA_{60}), and Poly(EA_{20}-$UPy_{3.75}$)-*b*-(EA_{60})-*b*-(EA_{20}-$GMA_{3.75}$).

Table S1. Theoretical M_n, experimental M_n, and Đ for polymers in this study.

Polymers	Conversion [%]	M_n^{Theo} x 10^4	M_n^{SEC} x 10^4	Đ
Poly[EA_{100}-UPy_5]	>95	1.25	1.62	1.19
Poly[EA_{100}-FMA_5]	80	1.12	1.17	1.23
Poly[EA_{100}-$UPy_{7.5}$]	>95	1.35	1.48	1.17
Poly[EA_{100}-$FMA_{7.5}$]	78	1.16	1.11	1.31
Poly[EA_{150}-$UPy_{11.25}$]	>95	2.00	1.32	1.18
Poly[EA_{150}-$FMA_{11.25}$]	81	1.73	1.68	1.25
Poly[EA_{20}-$Uy_{3.75}$]	>95	0.39	0.34	1.24
Poly[EA_{20}-$Uy_{3.75}$]-*b*-[EA_{60}]	>95	0.99	0.84	1.36
Poly[EA_{20}-$Uy_{3.75}$]-*b*-[EA_{60}]-*b*-[EA_{20}-$UPy_{3.75}$]	>95	1.35	1.62	1.34
Poly[EA_{20}-$UPy_{3.75}$]-*b*-[EA_{60}]-*b*-[EA_{20}-$FMA_{3.75}$]	78	1.26	1.54	1.31
Poly[EA_{20}-$UPy_{3.75}$]-*b*-[EA_{60}]-*b*-[EA_{20}-$GMA_{3.75}$]	>95	1.25	1.45	1.39

Table S2. Glass transition temperatures (T_g) of materials in this study.

Entry	DPN Designation	T_g [°C]
1	IPN-Lin$_{100}$UPy$_{5}$FMA$_{5}$0%CNT	-4.2±0.7
2	IPN-Lin$_{100}$UPy$_{5}$FMA$_{5}$0.5%CNT	-4.9±0.2
3	IPN-Lin$_{100}$UPy$_{5}$FMA$_{5}$1%CNT	-3.8±0.1
4	IPN-Lin$_{100}$UPy$_{7.5}$FMA$_{7.5}$0%CNT	-0.6±0.1
5	IPN-Lin$_{100}$UPy$_{7.5}$FMA$_{7.5}$1%CNT	0.9±0.1
6	IPN-Lin$_{100}$UPy$_{7.5}$FMA$_{7.5}$2.5%CNT	2.15±0.1
7	IPN-Lin$_{100}$UPy$_{7.5}$FMA$_{15}$0%CNT	-0.3±0.7
8	IPN-Lin$_{100}$UPy$_{7.5}$FMA$_{15}$1%CNT	1.1±0.1
9	IPN-Lin$_{100}$UPy$_{15}$FMA$_{7.5}$0%CNT	1.9±0.4
10	IPN-Lin$_{100}$UPy$_{15}$FMA$_{7.5}$1%CNT	0.8±0.03
11	IPN-Lin$_{100}$UPy$_{11.25}$FMA$_{11.25}$0%CNT	-1.2±0.0
12	IPN-Lin$_{100}$UPy$_{11.25}$FMA$_{11.25}$1%CNT	3.4±0.1
13	BCN-Blk$_{100}$UPy$_{7.5}$0%CNT	-4.1±0.1
14	BCN-Blk$_{100}$UPy$_{7.5}$1%CNT	-5.0±0.1
15	BCN-Blk$_{100}$UPy$_{3.75}$FMA$_{3.75}$0%CNT	-7.1±0.02
16	BCN-Blk$_{100}$UPy$_{3.75}$FMA$_{3.75}$1%CNT	-6.7±0.1
17	BCN-Blk$_{100}$UPy$_{3.75}$GMA$_{3.75}$0%CNT	-6.79±0.1
18	BCN-Blk$_{100}$UPy$_{3.75}$GMA$_{3.75}$1%CNT	-6.28±0.1

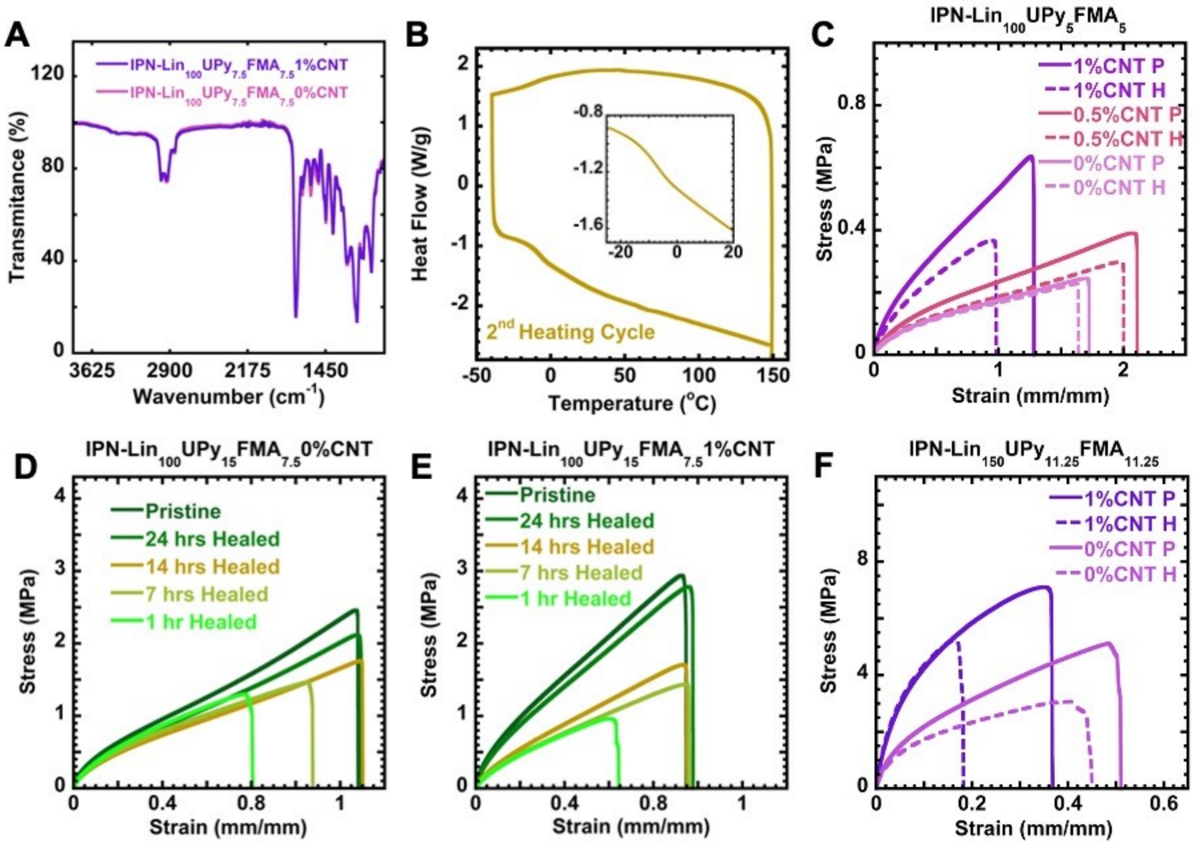

å

Figure S3. (**A**) Typical IR spectra for reinforced and reinforced IPN-Lin$_{100}$UPy$_{7.5}$FMA$_{7.5}$. (**B**) Typical DSC plot of DPNs using a BCN-Blk$_{100}$UPy$_{7.5}$0%CNT sample. (**C**) Stress-strain tensile testing of mechanical properties for IPN-Lin$_{100}$UPy$_{5}$FMA$_{7.5}$. (**D**) Time evolution self-healing of IPN-Lin$_{100}$UPy$_{15}$FMA$_{7.5}$0%CNT and (**E**) IPN-Lin$_{100}$UPy$_{15}$FMA$_{7.5}$1%CNT. (**F**) Stress-strain tensile testing of mechanical properties for IPN-Lin$_{150}$UPy$_{11.25}$FMA$_{11.25}$.

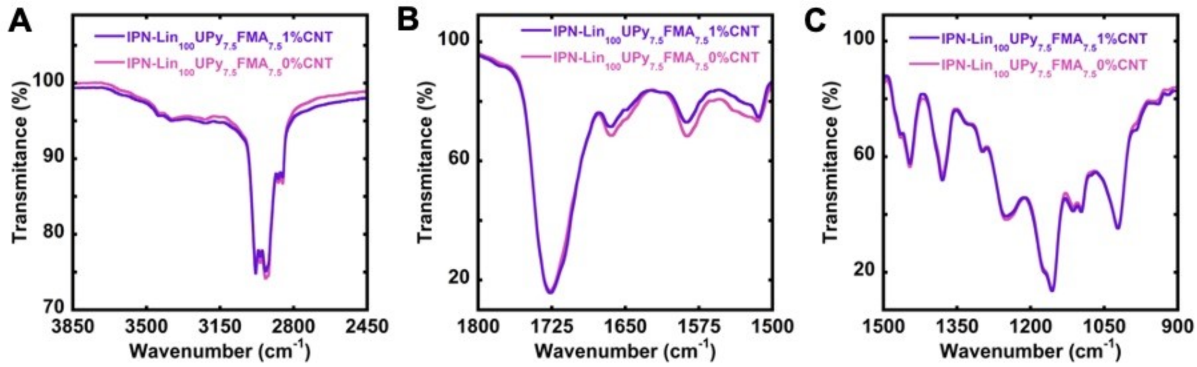

Figure S4. Closer look (zoomed-in) IR spectrum for reinforced and unreinforced IPN-Lin$_{100}$UPy$_{7.5}$FMA$_{7.5}$ materials.

Table S3. Proposed peak assignments for IR spectra of IPN-Lin$_{100}$UPy$_{7.5}$FMA$_{7.5}$ from Figure S3(A) and Figure S4(A-C).

Peak (cm^{-1})	Assignment
3500-3340	Secondary N–H Stretch
3550-2550	Carboxylic Acid O–H Stretch
3000-2800	C–H Alkene Stretch
1785-1700	C=O Ester Stretch
1700-1685	Conjugated Amide C=O Stretch
1600-1520	C=C Alkene stretch
1490-1440	C–H Scissor Bend
1390-1360	C–C Aliphatic Bend
1270-1200	C–O Asymmetric Stretch
1150-1100	Tertiary and Secondary C–O Ester Stretch
1025-1000	C–O–C Stretch

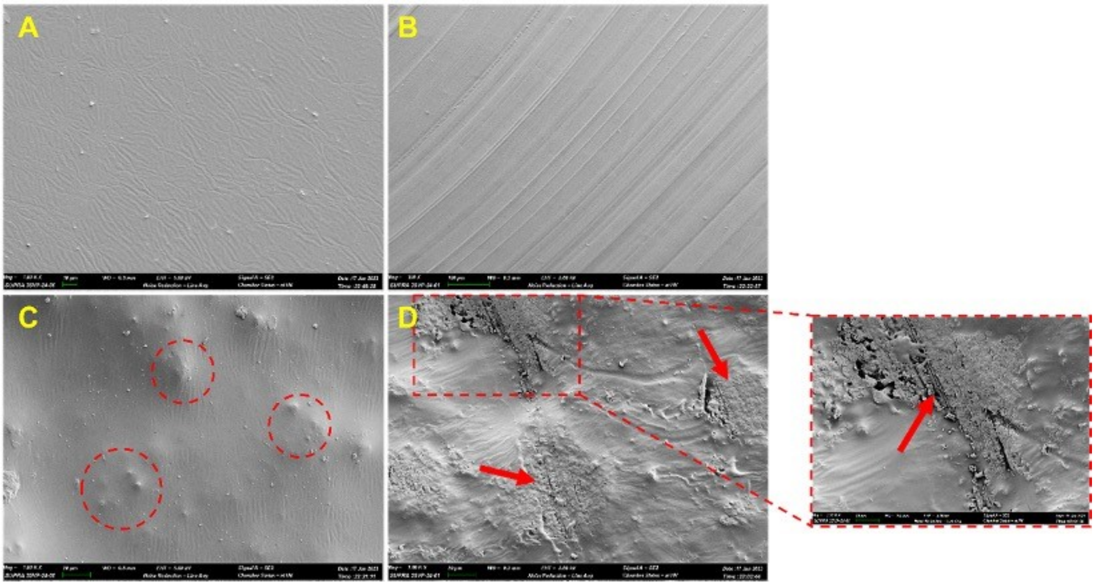

Figure S5. Scanning electron micrographs of (**A**) surface and (**B**) razor-sliced cross-section of IPN-$Lin_{100}UPy_{7.5}FMA_{7.5}$0%CNT. (**C**) Surface and (**D**) razor-sliced cross-section of IPN-$Lin_{100}UPy_{7.5}FMA_{7.5}$2.5%CNT.

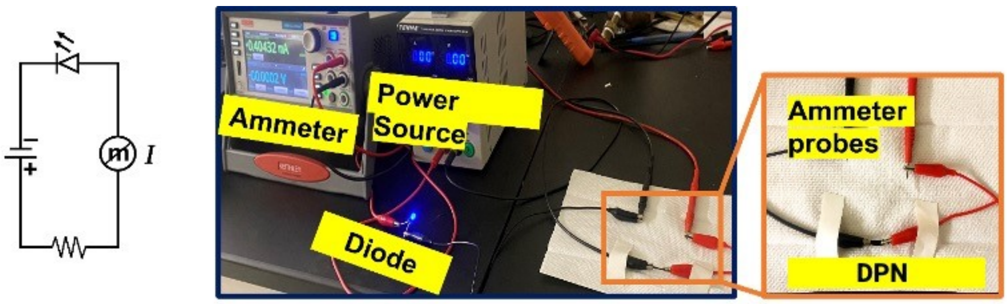

Figure S6. Electrical circuit and set-up for measuring current flowing through the circuit using IPN-$Lin_{100}UPy_{7.5}FMA_{7.5}$2.5%CNT as DPN

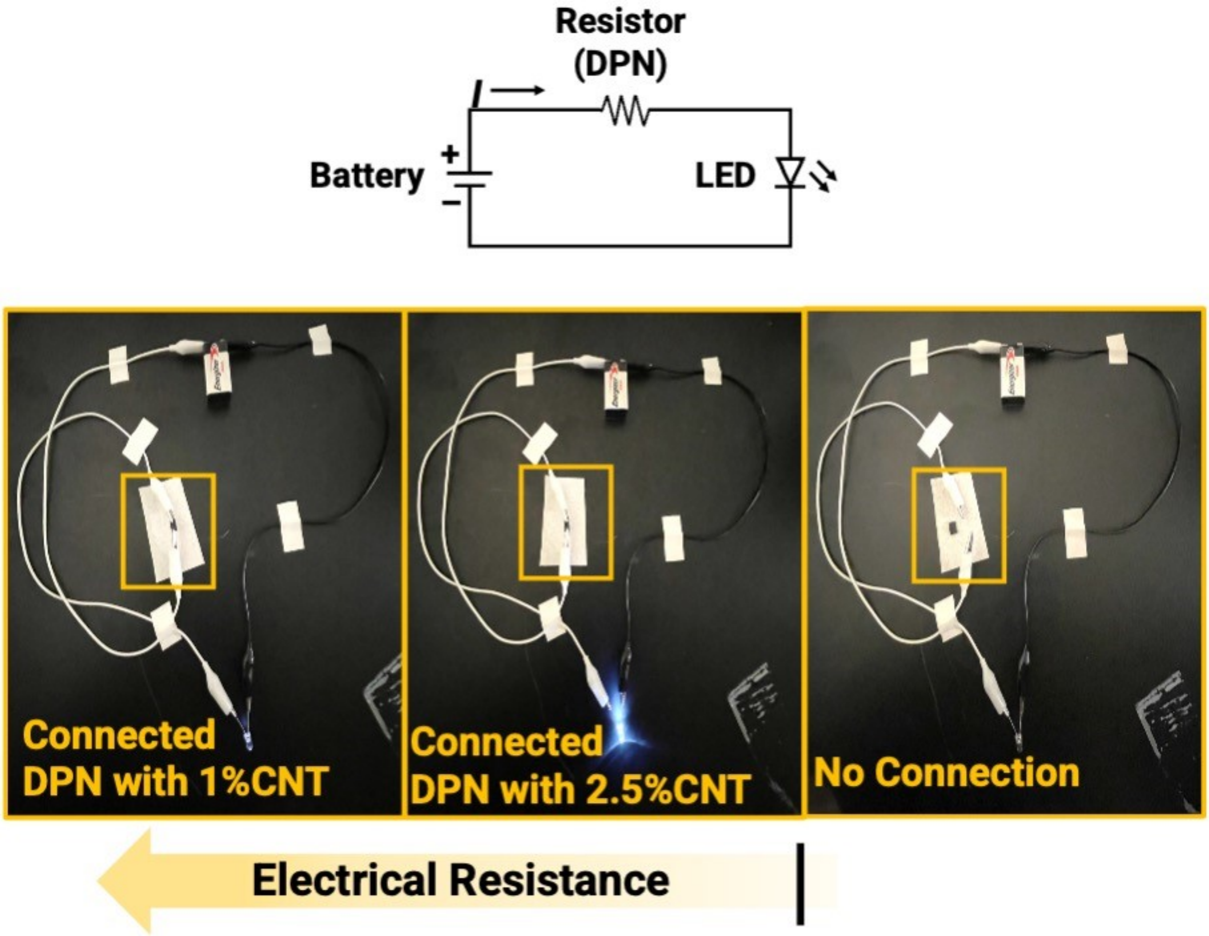

Figure S7. Impact of CNT loading on the electrical resistance of IPN-$Lin_{100}UPy_{7.5}FMA_{7.5}$ as DPN in a circuit system.

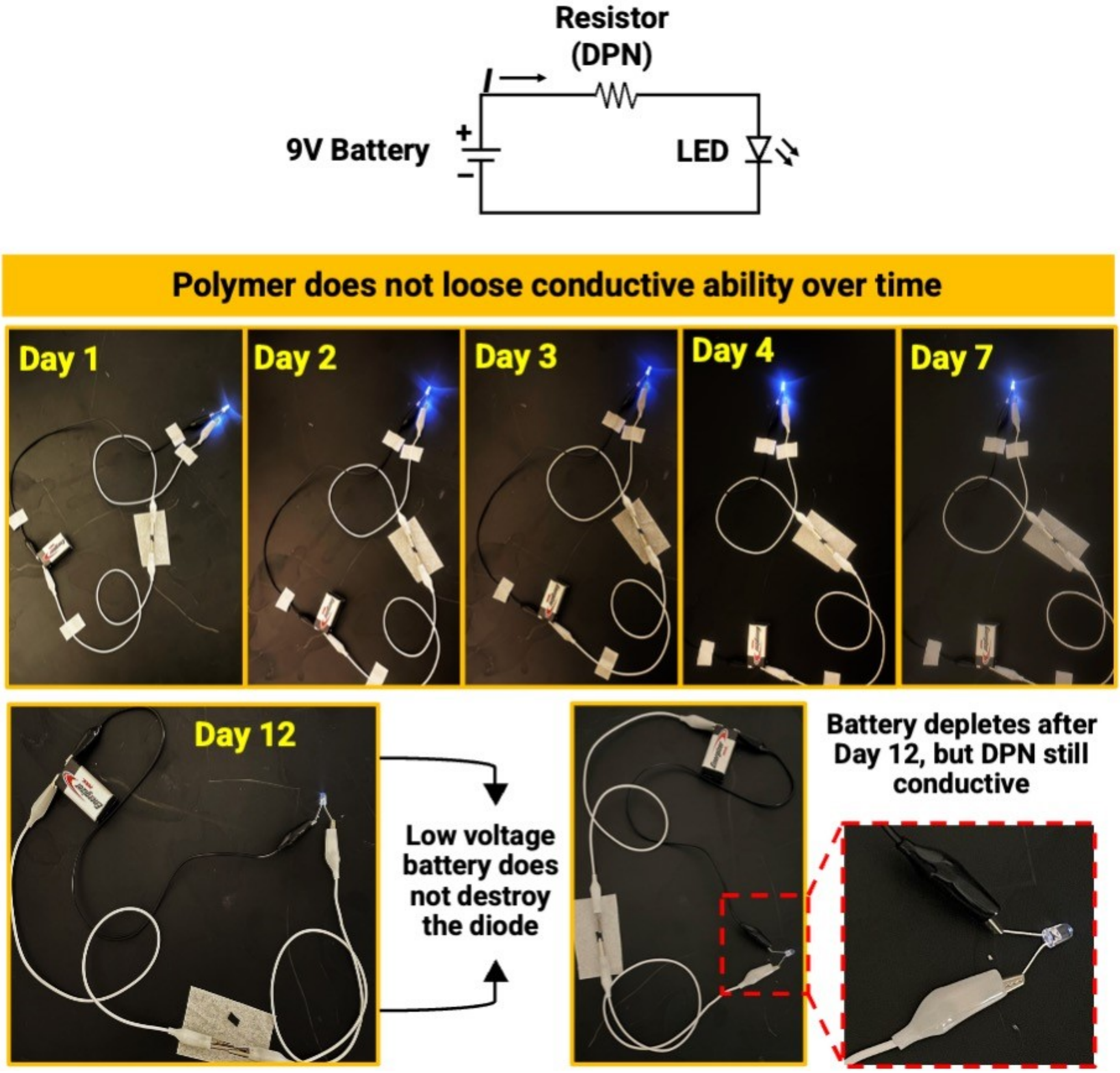

Figure S8. Conduction of current through IPN-Lin$_{100}$UPy$_{7.5}$FMA$_{7.5}$2.5%CNT in a circuit system which lasted until circuit battery was depleted.

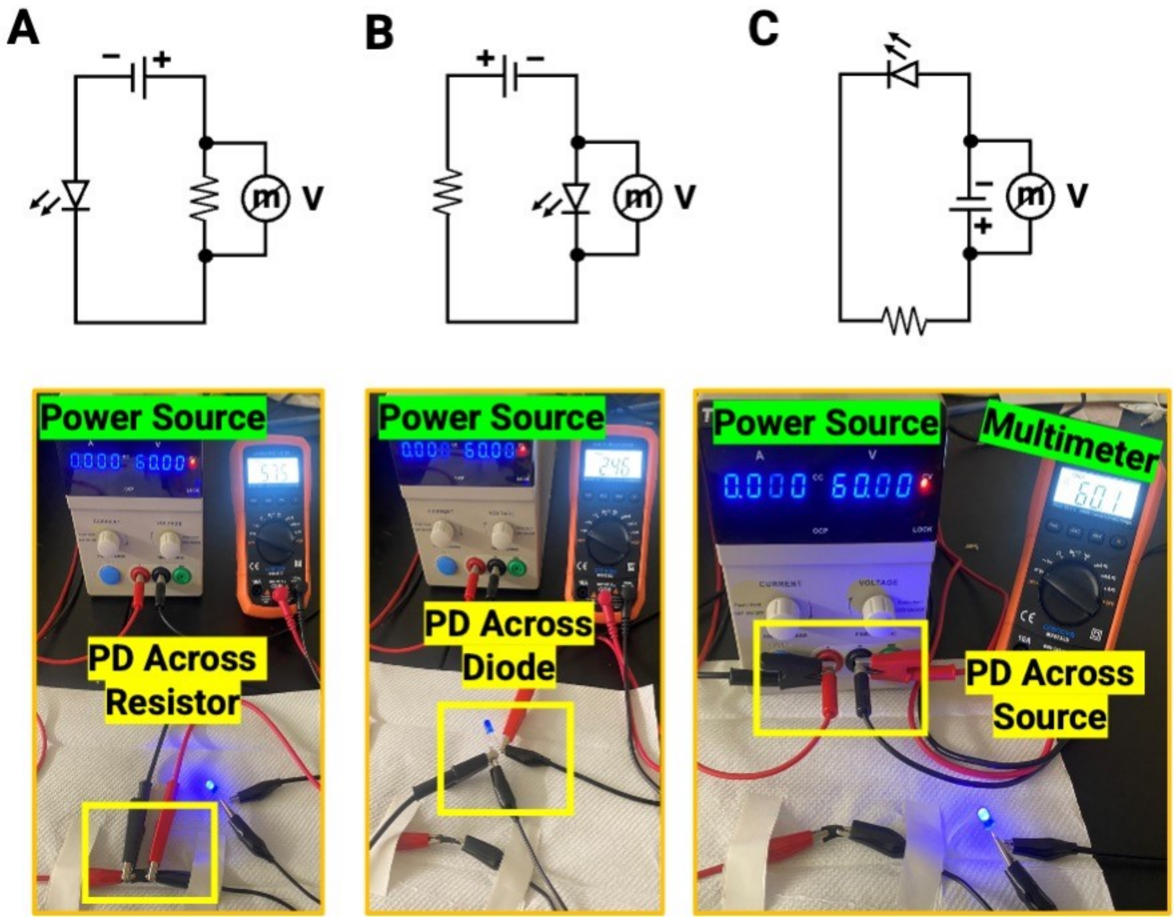

Figure S9. Electrical circuits and set-ups showing measurements of PD across (**A**) resistor, (**B**) diode, and (**C**) source.

Table S4. Verifying PD in IPN-Lin$_{100}$UPy$_{7.5}$FMA$_{7.5}$2.5%CNT using circuit set-ups as shown in Figure S9.

PD Across Source [V]	PD Across Resistor [V]	PD Across Diode [V]	PD [V] Across [Resistor + Diode]
10.00	07.56	02.45	10.01
20.00	17.57	02.44	20.01
30.00	27.50	02.49	29.99
40.00	37.50	02.51	40.01
50.00	47.50	02.50	50.00
60.00	57.50	02.52	60.02

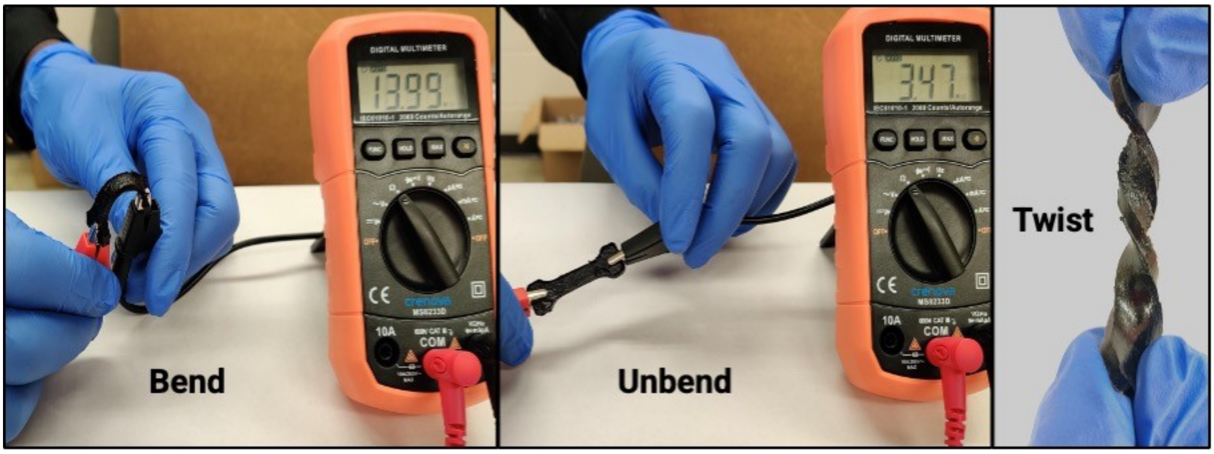

Figure S10. IPN-Lin$_{100}$UPy$_{7.5}$FMA$_{7.5}$2.5%CNT attached to a multimeter with bending and unbending photographs. Also twisted IPN-Lin$_{100}$UPy$_{7.5}$FMA$_{7.5}$2.5%CNT is shown with good flexibility.

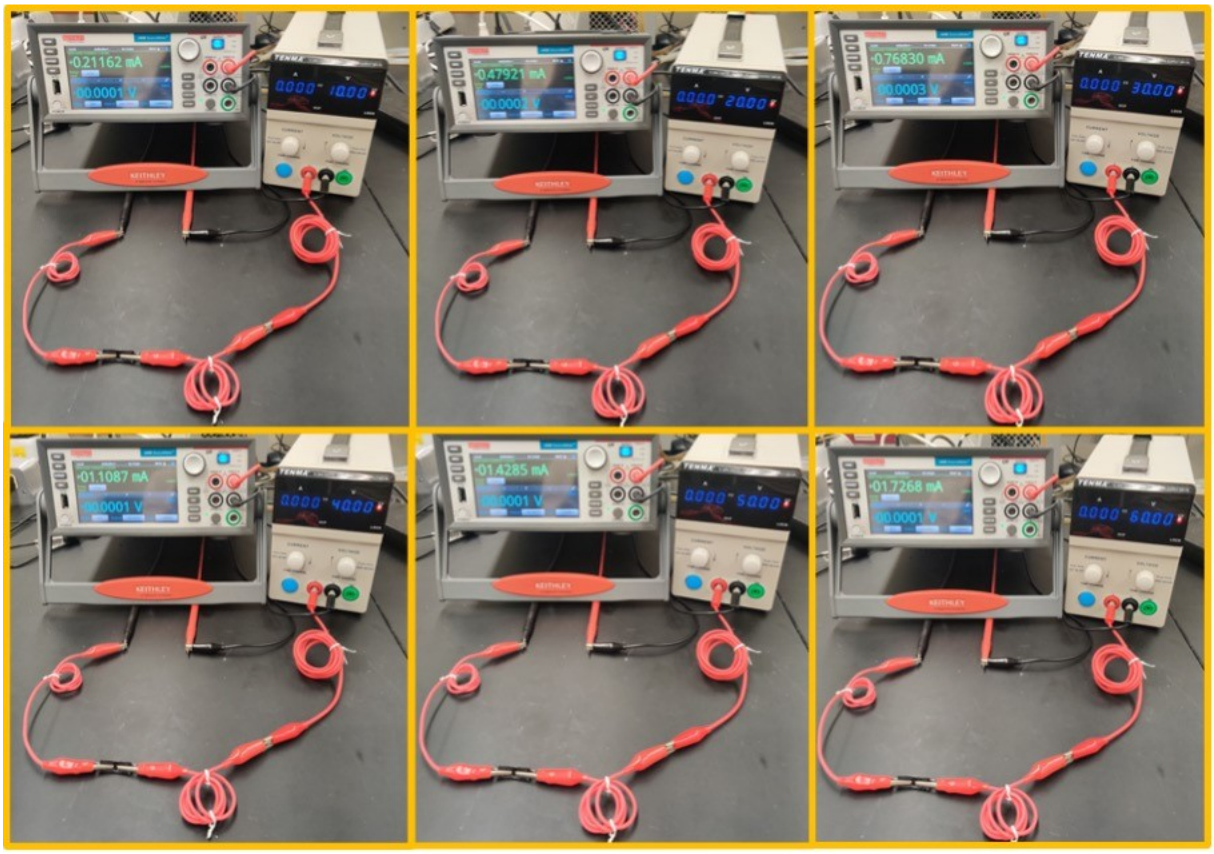

Figure S11. Typical set-up for measuring the impact of current on custom resistors using 30%L-70%H with applied voltage of 10, 20, 30, 40, 50, 60 V to obtain current-voltage plot.